Deformation Monitoring of Slopes by Vision Metrology with a Simulator for Network Design and the Hypothetical Test

Susumu Hattori, Japan, Yoshiyuki Ohnishi, Japan and Izuru Kuronuma, Japan

Key words: Deformation measurement, Displacement, Target, Photogrammetry, Hypothetical test, Observation Network

SUMMARY

The paper discusses the formulation and a procedure of deformation monitoring of slopes along highways or at quarries by use of vision metrology. A target field set at a slope is multi-exposed by a digital camera at appropriate epochs of time. Two sets of images taken at different epochs are simultaneously adjusted and tested hypothetically on whether any target is displaced or not between the exposures. The feasible design of an observation network is looked for a priori by simulation.

The network should be so configured that (1) it yields the object s coordinates of targets with high precision and (2) possesses the sensitivity enough for deformation detection. The latter criterion is derived from balanced probabilities of the first and the second kind error in judgment.

The paper formulates the hypothetical test procedure. For the purpose, Baarda’s Data Snooping is effectively applied. His technique is known as a method of gross error detection, where a blunder behaves equivalently to a displacement of a target. The formulation is validated by a simulator followed by an experiment.

要旨

高速道路や石切り場での変位検知を写真測量で行うための方法と必要な関係式を導いた。斜面に置いたターゲット場を適当な時間のエポックで多重撮影する。2 つの時間のエポックの写真群を同時調整して，どれか動いたターゲットがないかを検定する。適切な観測の網は前もってシミュレータで設計しておく。

観測の網は(1)ターゲットの空間座標が精度よく求められること。(2)変位検知ができるだけの十分な感度があること　を満たすように作る必要がある。後者の基準は第 1 種と第 2 種の判断の誤り確率がバランスしているという条件から導かれる。

仮説検定の手続きを導いたが，それにはよく知られた Baarda のデータスヌーピングを効果的に応用している。これは大誤差の検知に用いる方法であるが，ターゲットの変位と大誤差は同じふるまいをすることを利用した。導いた方法が正しいことをシミュレーションとそれに対応する実験で確認した。

Deformation Monitoring of Slopes by Vision Metrology with a Simulator for Network Design and the Hypothetical Test

Susumu Hattori, Japan, Yoshiyuki Ohnishi, Japan and Izuru Kuronuma, Japan

1. INTRODUCTION

Deformation of slopes along a highway or at a quarry should be observed periodically for disaster prevention. In many cases a total station (TS) is used for this purpose. Measurement with a TS, however, has such shortcomings as
(1) Time consuming for many targets,
(2) Occasionally no rooms to place a TS, and
(3) Hard a posteriori evaluation of measurement precision.

This paper discusses a photogrammetric method for deformation monitoring. Targets located at a slope are multi-disposed by a digital camera. Two Image sets obtained at different epochs of time are simultaneously adjusted to see whether any point is displaced between the epochs. Since relative movements of object points are observed, no fixed control points are required. Since the required order of deformation is almost the same as by photogrammetry, the hypothetical test is employed [Miura, 2004].

As other alternatives for displacement detection, an optical fiber displacement gauge[Suzuki, 2007] and systems using GPS already have been on market. These products are in principle make the autonomous works possible even at nights and in a bad weather, while photogrammety is more advantageous with respect to cost.

An appropriate observation network is designed by a simulator before targets are placed. This paper discusses mathematical aspects of deformation detection by photogrammetry and functions of the simulator. An experimental result is shown to validate the discussion.

*Section two shows a typical slope and an observation configuration for better perspective.
*Section three is devoted to outline of adjustment in photogrammetric measurements and a hypothetical test for deformation detection. A target field on a slope is exposed at two epochs of time, and the two sets of image coordinates of targets are simultaneously bundle-adjusted to obtain object coordinates of the targets, which are then tested to detect whether any point is displaced by the method based on Baarda's data snooping [Baarda, 1968].
*Section four introduces a simulator developed for designing network configuration. That is, where the targets should be placed and how many photographs should be taken, are considered a priori to obtain the required sensitivity of detection.
* Section five shows some experimental results to validate the discussion.

2. A MODEL OF A SLOPE AND A CAMERA CONFIGURATION

Fig1 shows a typical slope along a high-way and a targets and camera configuration. The X axis is taken along a slope, the Y axis is to the vertical and the Z axis to complete the right hand system. Generally possible camera positions would be limited due to topography. For example exposures downwards from high position might be impossible. Hence a camera configuration that the slope is exposed at stations on a straight line along a lane, sighting on a level or upwards is considered. This configuration is not preferable but practical.

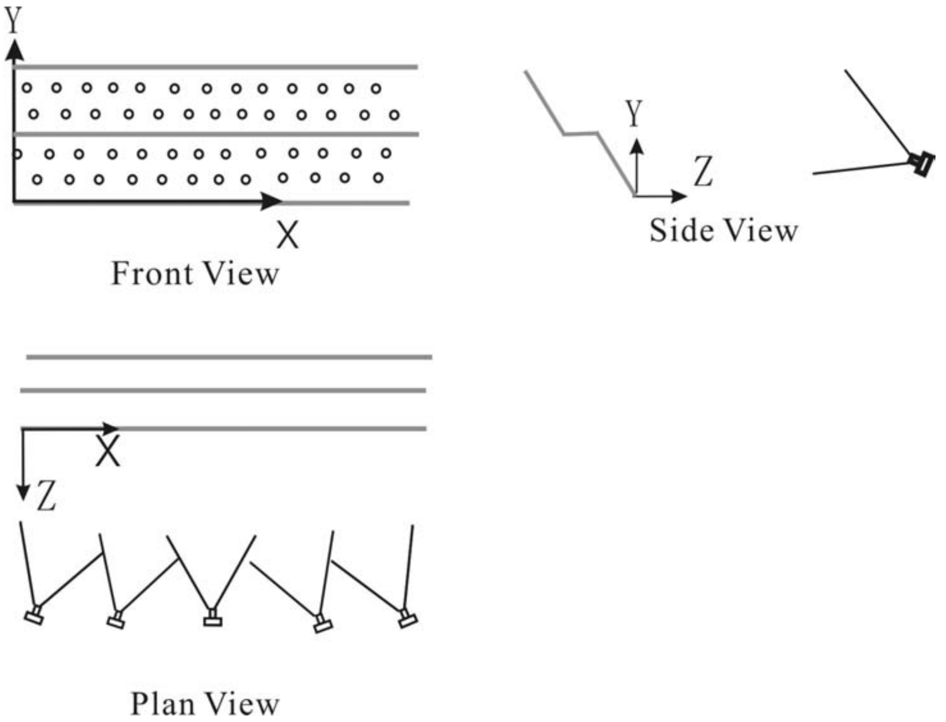

Fig.1 Schematic view of a typical slope and a camera configuration

3. THE STRENGTH OF A PHOTOGRAMMETRIC NETWORK

3.1 General

The criteria of a good photogrammetric network to detect deformation are (1) precision of adjusted object coordinates of targets, (2) sensitivity of detection and (3) stability to single out outliers [Benzao, 1995, Miura,2005]. Since in photogrammetric networks many targets are simultaneously observed, the third condition is automatically met if the first and second conditions are met.

3.2 Precision of object coordinates of targets obtained by bundle adjustment of images

The precision (or standard deviation) of object coordinates of targets is given by the variance covariance matrix of object coordinates. The standard deviations of object coordinates must be smaller than minimal displacement required to be detected.

The relation between image coordinates and object coordinates is expressed by the well-known collinearity equations.

$$x + \Delta x = -c\frac{m_{11}(X - X_0) + m_{12}(Y - Y_0) + m_{13}(Z - Z_0)}{m_{31}(X - X_0) + m_{32}(Y - Y_0) + m_{33}(Z - Z_0)} \tag{1}$$

$$y + \Delta y = -c\frac{m_{21}(X - X_0) + m_{22}(Y - Y_0) + m_{23}(Z - Z_0)}{m_{31}(X - X_0) + m_{32}(Y - Y_0) + m_{33}(Z - Z_0)} \quad ,$$

where c is a camera constant, $\Delta x, \Delta y$ are corrections to lens distortions and principal point coordinates. $M = (m_{ij})$ is a rotation matrix. $\mathrm{O}(X_0, Y_0, Z_0)$ is the projection center (refer to Fig.2). The system of observation equations obtained by linearizing (1) and set up for all mage coordinates is expressed as

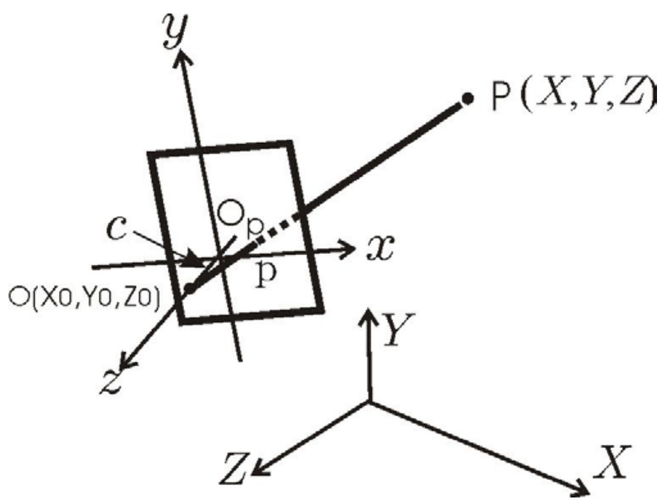

Fig.2 Image coordinate system and object space coordinate system

$$\mathbf{v} = \mathbf{A}_1\mathbf{x}_1 + \mathbf{A}_2\mathbf{x}_2 + \mathbf{A}_3\mathbf{x}_3 + \mathbf{e} : \quad \mathbf{P} \tag{2}$$

or

$$\mathbf{v} = \mathbf{A}\mathbf{x} + \mathbf{e} \quad : \mathbf{P} \tag{2'}$$

$$\mathbf{A} = \left[\mathbf{A}_1 \ \mathbf{A}_2 \ \mathbf{A}_3\right], \quad \mathbf{x}^T = \left[\mathbf{x}_1^T \ \mathbf{x}_2^T \ \mathbf{x}_3^T\right]$$

Where $\mathbf{A}$ is a design matrix, $\mathbf{x}$ is a unknown parameters vector, $\mathbf{e}$ is a discrepancy vector and $\mathbf{P}$ is a weight matrix. Suffixes 1, 2 and 3 mean exterior, interior orientation parameters and object coordinates respectively. Interior orientation parameters are also treated as unknowns and estimated by self calibration. As lens distortions Brown parameters are employed [Brown,1966].

(2') is solved by free network, since no control points are given. Let seven vectors denoted by

$$\mathbf{G}^T = \left[\mathbf{G}_1^T \ \ \mathbf{G}_2^T \ \ \mathbf{G}_3^T\right] \quad , \tag{3}$$

which are orthogonal to row vectors of $\mathbf{A}$ and to one another as well (called orthogonal basis matrix). Among the least squares solutions the vector that minimizes the mean variance of object coordinates is given by

$$\hat{\mathbf{x}} = \left(\mathbf{A}^T\mathbf{P}\mathbf{A} + \mathbf{B}\mathbf{B}^T\right)^{-1}\mathbf{A}^T\mathbf{P}\mathbf{e} \tag{4}$$

and its variance-covariance matrix is given by

$$\mathbf{\Sigma}_{\hat{x}} = \hat{\sigma}_0^2\left((\mathbf{A}^T\mathbf{P}\mathbf{A} + \mathbf{B}\mathbf{B}^T)^{-1} - \mathbf{G}(\mathbf{G}^T\mathbf{B}\mathbf{B}^T\mathbf{G})^{-1}\mathbf{G}^T\right) \tag{5}$$

$$\hat{\sigma}_0^2 = \hat{\mathbf{v}}^T\mathbf{P}\hat{\mathbf{v}}/(m - n + 7) \tag{6}$$

where $\hat{\sigma}_0^2$ is a posteriori observation variance of image coordinates.

3.3 Sensitivity of the network for deformation detection

Since the order of errors included in object coordinates of targets and that of required detectable displacements are not differ largely, detection is based on the hypothetical test. The procedure is as follows: The target field is exposed at two epochs of time. For each target point the null hypothesis that no displacements occur between the epochs is tested against the alternative hypothesis that displacement occurs. And if estimated displacement is significant, the null hypothesis is rejected. Due to correlation between object coordinates of two targets, detection sensitivity might degrade, if the disposition of targets and exposure configurations are not appropriate.

In the test the first and second kind of errors in judgment must be balanced and small enough. Fig. 3 shows a schematic diagram of the first and second kind judgment error. When the null hypothesis holds, a statistics is subject to the distribution $F(T,f)$ with a degree of freedom f. And when the alternative hypothesis holds, the statistics is subject to the distribution $F'(T,f,\delta^2)$, where δ^2 is a non-centrality parameter. The first kind error probability α and the second kind error probabilities $1-\beta$ should be balanced at a threshold T_B which is determined by the simulator.

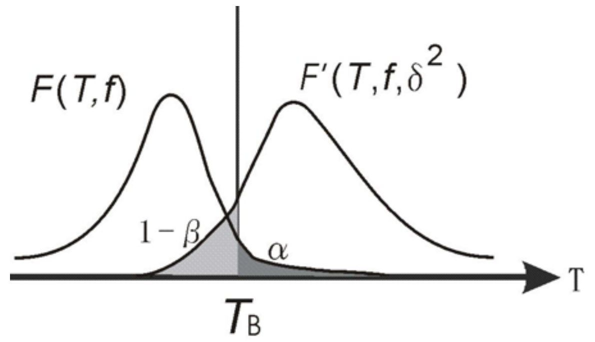

Fig.3 Schematic diagram of the first and second kind error

In the following two epochs of time are differentiated by I,II. Observation equations in I and II are combined as

$$\begin{bmatrix} \mathbf{v}_{\mathrm{I}} \\ \mathbf{v}_{\mathrm{II}} \end{bmatrix} + \begin{bmatrix} \mathbf{A}_{1,\mathrm{I}} & \mathbf{0} & \mathbf{A}_{2,\mathrm{I}} & \mathbf{0} & \mathbf{A}_{3,\mathrm{I}} \\ \mathbf{0} & \mathbf{A}_{1,\mathrm{II}} & \mathbf{0} & \mathbf{A}_{2,\mathrm{II}} & \mathbf{A}_{3,\mathrm{II}} \end{bmatrix} \begin{bmatrix} \mathbf{x}_{1,\mathrm{I}} \\ \mathbf{x}_{1\mathrm{1II}} \\ \mathbf{x}_{2,\mathrm{I}} \\ \mathbf{x}_{2,\mathrm{II}} \\ \mathbf{x}_{3} \end{bmatrix} = \begin{bmatrix} \mathbf{e}_{\mathrm{I}} \\ \mathbf{e}_{\mathrm{II}} \end{bmatrix} \qquad \mathbf{P} = \begin{bmatrix} \mathbf{P}_{\mathrm{I}} & 0 \\ 0 & \mathbf{P}_{\mathrm{II}} \end{bmatrix} \tag{7}$$

Note that suffixes are differently defined from (2). The vectors $\mathbf{x}_{1,\mathrm{I}}, \mathbf{x}_{1,\mathrm{II}}$ are exterior and interior orientation parameters. And the $\mathbf{x}_{2,\mathrm{I}}, \mathbf{x}_{2,\mathrm{II}}$ are object coordinates vectors of the targets imaged only in epoch I, and in epoch II respectively. The $\mathbf{x}_3$ is object coordinates vector imaged in I and II commonly. The weight matrix $\mathbf{P}_{\mathrm{I}}$ is usually a unit, and $\mathbf{P}_{\mathrm{II}}$ is scaled to $\mathbf{P}_{\mathrm{I}}$. (7) can also be expressed concisely

$$\mathbf{v} + \mathbf{AX} = \mathbf{e} : \mathbf{P} \tag{7'}$$

Correspondence of symbols between (7) and (7') is apparent. In the unknown parameters vector $\mathbf{X}$ object coordinates are assumed to be arranged in the order of X, Y, Z for each target.
The displacement for Target k (k=1,2,,,,K) is estimated in the following. Let the displacement vector be denoted by

$$\mathbf{\Delta} = \left[\mathit{\Delta}_X \ \mathit{\Delta}_Y \ \mathit{\Delta}_Z\right]^T, \tag{8}$$

and then (7) can be modified as,

$$\begin{bmatrix} \mathbf{v}_{\mathrm{I}} \\ \mathbf{v}_{\mathrm{II}} \end{bmatrix} + \begin{bmatrix} \mathbf{A}_{1,\mathrm{I}} & \mathbf{0} & \mathbf{A}_{2,\mathrm{I}} & \mathbf{0} & \mathbf{A}_{3,\mathrm{I}} & \mathbf{0} \\ \mathbf{0} & \mathbf{A}_{1,\mathrm{II}} & \mathbf{0} & \mathbf{A}_{2,\mathrm{II}} & \mathbf{A}_{3,\mathrm{II}} & \mathbf{A}_{3,\mathrm{II}}\widetilde{\mathbf{J}}_k \end{bmatrix} \begin{bmatrix} \mathbf{x}_{1,\mathrm{I}} \\ \mathbf{x}_{11\mathrm{II}} \\ \mathbf{x}_{2,\mathrm{I}} \\ \mathbf{x}_{2,\mathrm{II}} \\ \mathbf{x}_3 \\ \Delta \end{bmatrix} = \begin{bmatrix} \mathbf{e}_{\mathrm{I}} \\ \mathbf{e}_{\mathrm{II}} \end{bmatrix} : \quad \mathbf{P} = \begin{bmatrix} \mathbf{P}_{\mathrm{I}} & \mathbf{0} \\ \mathbf{0} & \mathbf{P}_{\mathrm{II}} \end{bmatrix} \tag{9}$$

where $\widetilde{\mathbf{J}}_k$ is a (3K,3) zero matrix, with the k'th block being replaced by a unit matrix; i.e.

$$\widetilde{\mathbf{J}}_k = \begin{bmatrix} 0 & 0 & 0 & \\ 0 & 0 & 0 & (1) \\ 0 & 0 & 0 & \\ \ddots & & & \\ & \ddots & & \\ & & \ddots & \\ 1 & 0 & 0 & \\ 0 & 1 & 0 & (k) \\ 0 & 0 & 1 & \\ \ddots & & & \\ & \ddots & & \\ & & \ddots & \\ 0 & 0 & 0 & \\ 0 & 0 & 0 & (K) \\ 0 & 0 & 0 & \end{bmatrix}. \tag{10}$$

With (10), (9) is written in the form

$$\mathbf{v} + \left[\mathbf{A} \ \ \mathbf{J}_k\right] \begin{bmatrix} \mathbf{X} \\ \mathbf{\Delta} \end{bmatrix} = \mathbf{e} : \mathbf{P} \tag{11}$$

with

$$\mathbf{J}_k = \begin{bmatrix} \mathbf{0} \\ \mathbf{A}_{\mathrm{II}}\widetilde{\mathbf{J}}_k \end{bmatrix} \tag{12}$$

The least square solution of (11) is given by

$$\begin{bmatrix} \hat{\mathbf{X}} \\ \hat{\boldsymbol{\Delta}} \end{bmatrix} = \begin{bmatrix} \mathbf{A}^{\mathrm{T}}\mathbf{PA} & \mathbf{A}^{\mathrm{T}}\mathbf{PJ}_k \\ \mathbf{J}_k^{\mathrm{T}}\mathbf{PA} & \mathbf{J}_k^{\mathrm{T}}\mathbf{PJ}_k \end{bmatrix}_{\mathrm{rs}}^{-} \begin{bmatrix} \mathbf{A}^{\mathrm{T}}\mathbf{Pe} \\ \mathbf{J}_k^{\mathrm{T}}\mathbf{Pe} \end{bmatrix} \tag{13}$$

The right hand side coefficient matrix can be expanded [Koch,1999] to

$$\begin{bmatrix} \mathbf{A}^{\mathrm{T}}\mathbf{PA} & \mathbf{A}^{\mathrm{T}}\mathbf{PJ}_k \\ \mathbf{J}_k^{\mathrm{T}}\mathbf{PA} & \mathbf{J}_k^{\mathrm{T}}\mathbf{PJ}_k \end{bmatrix}_{\mathrm{rs}}^{-} = \begin{bmatrix} (\mathbf{A}^{\mathrm{T}}\mathbf{PA})_{\mathrm{rs}}^{-}(\mathbf{E} + \mathbf{A}^{\mathrm{T}}\mathbf{PJ}_k\mathbf{SJ}_k^{\mathrm{T}}\mathbf{PA}(\mathbf{A}^{\mathrm{T}}\mathbf{PA})_{\mathrm{rs}}^{-}) & -(\mathbf{A}^{\mathrm{T}}\mathbf{PA})_{\mathrm{rs}}^{-}\mathbf{A}^{\mathrm{T}}\mathbf{PJ}_k\mathbf{S} \\ -\mathbf{SJ}_k^{\mathrm{T}}\mathbf{PA}(\mathbf{A}^{\mathrm{T}}\mathbf{PA})_{\mathrm{rs}}^{-} & \mathbf{S} \end{bmatrix} \tag{14}$$

$$\mathbf{S} = (\mathbf{J}_k^{\mathrm{T}}\mathbf{PQ}_{\hat{\mathrm{v}}}\mathbf{PJ}_k)^{-1}$$
$$\mathbf{Q}_{\hat{\mathrm{v}}} = \mathbf{P}^{-1} - \mathbf{A}(\mathbf{A}^{\mathrm{T}}\mathbf{PA})_{\mathrm{rs}}^{-}\mathbf{A}^{\mathrm{T}}$$

As the result the most probable values of displacement $\hat{\boldsymbol{\Delta}}$ is given by

$$\hat{\boldsymbol{\Delta}} = \mathbf{SJ}_k^{\mathrm{T}}\mathbf{PQ}_{\hat{\mathrm{v}}}\mathbf{Pe} = -\mathbf{SJ}_k^{\mathrm{T}}\mathbf{P}\hat{\mathbf{v}} \tag{15}$$

In the following, errors in image coordinate measurements are supposed to be distributed to normal with the mean 0 and the variance $\sigma_0{}^2$. The null hypothesis

$$\mathbf{H}_0 : \boldsymbol{\Delta} = \mathbf{0} \quad \text{or} \quad \mathbf{H}_0 : [\mathbf{0} \quad \mathbf{I}]\begin{bmatrix} \mathbf{X} \\ \boldsymbol{\Delta} \end{bmatrix} = \mathbf{0} \tag{16}$$

is tested against the alternative hypothesis

$$\mathbf{H}_{\mathrm{a}} : \boldsymbol{\Delta} = \hat{\boldsymbol{\Delta}} \neq \mathbf{0} \quad \text{or} \quad \mathbf{H}_{\mathrm{a}} : [\mathbf{0} \quad \mathbf{I}]\begin{bmatrix} \mathbf{X} \\ \boldsymbol{\Delta} \end{bmatrix} = \hat{\boldsymbol{\Delta}} \neq \mathbf{0} \tag{17}$$

If the null hypothesis is true, a test statistics

$$T_X = \left(R^2 / r\right)\sigma_0{}^2 \tag{18}$$

is subject to X^2 distribution , $\mathrm{X}^2(r)$, **if** σ^2 **is known**, where r is a degree of freedom =3. R is a variance that the diplacements of target P_k account for in the total variance

$$\Omega = \mathbf{e}^{\mathrm{T}}\mathbf{P}\mathbf{Q}_{\hat{\mathbf{v}}}\mathbf{P}\mathbf{e}\,, \tag{19}$$

R is reduced to

$$\begin{aligned} R &= \left(\begin{bmatrix} \mathbf{0} & \mathbf{E} \end{bmatrix} \begin{bmatrix} \hat{\mathbf{X}} \\ \hat{\boldsymbol{\Delta}} \end{bmatrix} \right)^{\mathrm{T}} \left(\begin{bmatrix} \mathbf{0} & \mathbf{E} \end{bmatrix} \begin{bmatrix} \mathbf{A}^{\mathrm{T}}\mathbf{PA} & \mathbf{A}^{\mathrm{T}}\mathbf{PJ}_k \\ \mathbf{J}_k^{\mathrm{T}}\mathbf{PA} & \mathbf{J}_k^{\mathrm{T}}\mathbf{PJ}_k \end{bmatrix}_{\mathrm{rs}}^{-} \begin{bmatrix} \mathbf{0} \\ \mathbf{E} \end{bmatrix} \right)^{-1} \left(\begin{bmatrix} \mathbf{0} & \mathbf{E} \end{bmatrix} \begin{bmatrix} \hat{\mathbf{X}} \\ \hat{\boldsymbol{\Delta}} \end{bmatrix} \right) \\ &= \hat{\boldsymbol{\Delta}}^{\mathrm{T}}\mathbf{S}^{-1}\hat{\boldsymbol{\Delta}} = \hat{\mathbf{v}}^{\mathrm{T}}\mathbf{PJ}_k\left(\mathbf{J}_k\mathbf{PQ}_{\hat{\mathbf{v}}}\mathbf{PJ}_k\right)^{-1}\mathbf{J}_k\mathbf{P}\hat{\mathbf{v}} \end{aligned} \tag{20}$$

A statistics T_α is determined for a given significant level α , The balanced threthold T_B is equal or larger than T_α .

If the alternative hypothesis is true, the test statistics T_X in (18) is subject to the non-central X^2 distributuion, $\mathrm{X}'^2(r,\delta^2)$, where δ^2 is a noncentrality parameter,

$$\delta^2 = \hat{\boldsymbol{\Delta}}^T\mathbf{J}_k^T\mathbf{PQ}_{\hat{\mathbf{v}}}\mathbf{PJ}_k\hat{\boldsymbol{\Delta}}/\sigma_\Delta^2\,. \tag{21}$$

where σ_Δ^2 is the a priori variance of image coordinate errors, when Δ is incorporated as is shown in (11).

If σ^2 **is unknown**, which is a rational assumption in field works, an a posteriori variance $\hat{\sigma}_0^2$ must be used instead. And the X^2 distributuion should be replaced by the F distribution. The statistics

$$T_F = \frac{R/r}{\Omega_\Delta/(m-(n+r)+7)} \tag{22}$$

is subject to the F distribution, $F\left(r, m-(n+r)+7\right)$, where m is a total number of observations, and n is the number of unknowns. $\Omega_\Delta = \Omega - R$ is a variance which all parameters but only the displacement Δ accounts for in the totall variance Ω .

4. SIMULATOR FOR NETWORK DESIGN

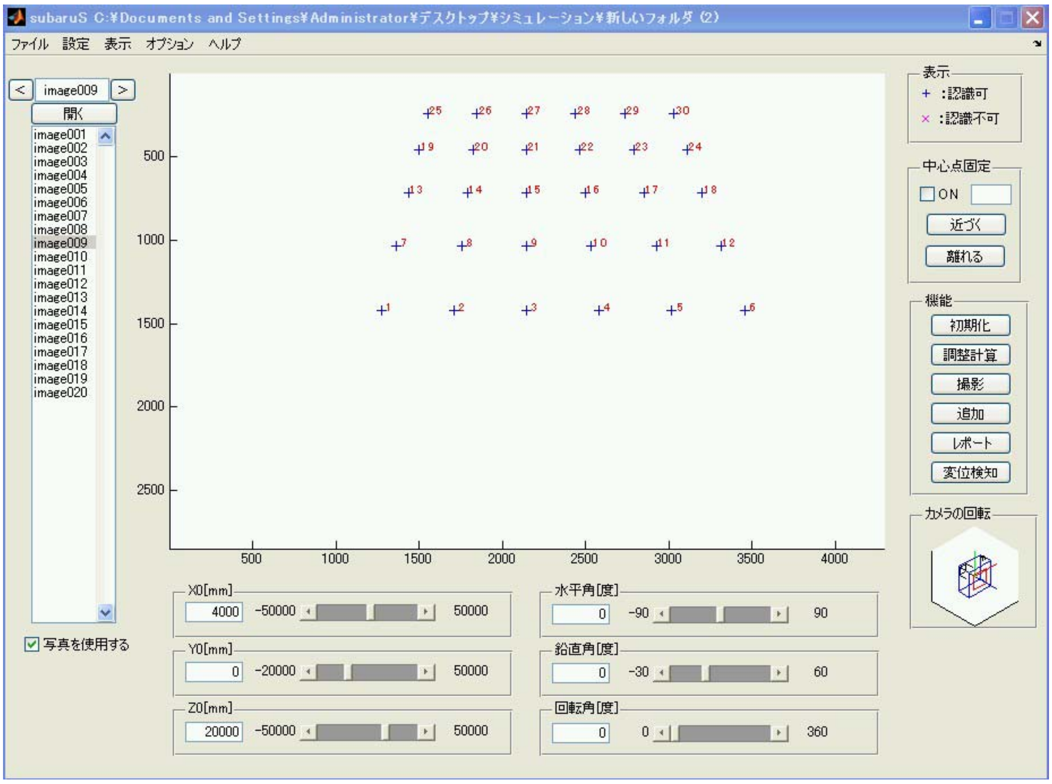

Fig.3 A screen of the simulator (see **5.2**)

4.1 Input of parameters

To compare feasible configurations of observation network, a computer simulator is developed. Fig.3 shows a screen example for an image for a simulation in 5.2. An operator is asked to input the following basic parameters;

(1) Area of the slope, its gradient and targeting spacing
(2) Size of the imaging sensor, its pixel width, focal length *c* of a camera
(3) Camera stations, number of exposures at each station
(4) A priori variance of image coordinates measurements σ^2**.** It depends on the quality of targets and the pixel width of the sensor.

4.2 Calculation of an expected precision

The simulator calculates the image coordinates for all the images by back drive. Ill posing exposures are warned. Then it calculates the expected variance of the object coordinates of targets (upper left window of Fig. 6) .

4.3 Calculation of expected sensitivity

4.3.1 Sensitivity to the first kind error

The simulator calculates the sensitivity of the network to the first kind error. In simulation a priori variance of image coordinates, σ^2 is always known. Therefore for a given condition a statistics T_α subject to the X^2 distribution for a prescribed significant level α is looked for. Typically α is set to 5%. Then the variance of detectable displacements is calculated from (18) as

$$R = \sqrt{T_\alpha \, r/\sigma^2} \quad . \tag{27}$$

The detectable displacement Δ is three-dimensional. Though it is possible to give the direction and magnitude simultaneously, it might be simple and practical to divide it to the Y and Z directions independently, i.e. Δ_Y and Δ_Z.

Then from (25) the displacement to Y only is

$$\Delta_Y = \sqrt{R/\overline{S}_{2,2}} \tag{28}$$

where $\overline{S}_{2,2}$ means the (2,2) element of matrix $\mathbf{S}^{-1}$. Likewise

$$\Delta_Z = \sqrt{R/\overline{S}_{3,3}} \tag{29}$$

4.3.2 Sensitivity to the second kind error

On the other hand, the second kind error must be also considered. For prescribed power β (typically set to 0.8), the set of Δ_Y (or Δ_Z) and T_β, which is larger than T_α and satisfies

$$\mathrm{X}'^2\,(T_\beta, r, \delta^2) \le 1-\beta, \tag{30}$$

are looked for. This value of T_β is adopted as a balanced threshold T_B. If T_F in (26) is larger than T_B for a given significant level α and a power β, the null hypothesis is rejected (or Target *k* is judged to be displaced) .

5. A SIMULATION AND AN EXPRIMENT

5.1 General

A set of a simulation and an experiment are conducted at a small slope as shown in Fig.4. The camera used is NikonD90 (3K*4K) with 24 mm fixed focal lens. A priori precision of image coordinates is set to 1/10 pixel = 0.6 μ m. Fig. 6.1 shows the experimental site. Six targets in X and five targets in Y, with two meter spacing, are placed. This spacing is too small for actual use. This is because the experiment slope is small, and 15-20 targets are necessary for stable self calibration. Along the slope four images are exposed at five stations. Distance to the object space is about 20m.

5.2 Simulation result

Fig.3 is an example of a simulated image exposing the target field. Table 1 shows expected precision (standard deviation) in X, Y and Z, where the detection thresholds obtained are 1mm in Y and 2.5-3mm in X and Z. It is noted that the sensitivity in Y is better than in X or Z. This fact is very convenient for displacement detection in a slope, since most of displacement at an early stage is expected to occur downwards.

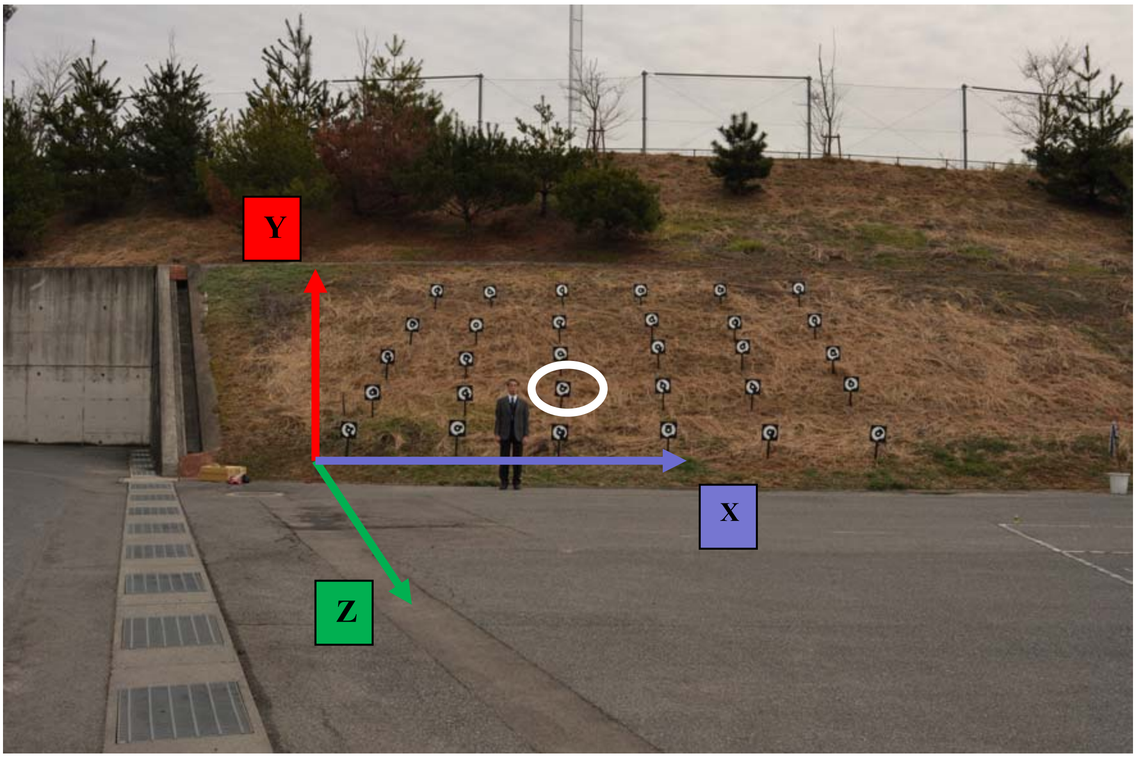

Fig. 4 Experiment site
A circle designates a target displaced between two epochs of time

Table 1 Expected precision of object coordinates of targets in simulation

Standard deviaions (mm)			
X	*Y*	*Z*	rms
0.574	0.392	0.596	0.529

5.2 Experimental result

At the first epoch of time, twenty images are exposed with the above digital camera in total conformity with the simulation condition, except for interior orientation parameters. In simulation they are all set to zero. At each station the camera is rotated by 90° to determine interior orientation parameters accurately and to make use of all corners of the screen uniformly. Sensor sensitivity is set at 200 (ISO), aperture at 9 and shutter speed at 1/250 second. Target size is 50mm in diameter. The targets are provided with a ring codes for automatic numbering as shown in Fig5.The target centers are measured up to 1/100pixel by image processing. Targets are made of epoxy resin, different from retro targets for industrial use, since bright reflectance hampers safe traffics [Hattori, 2002].

Fig.5 Coded targets for automatic numbering

All the images in the first epoch are bundle-adjusted. Table 2 shows the precision of object coordinates of the targets. The precision is about twice higher than in the simulation. This means the performance of the targets is under-evaluated. According to other experiments, this performance holds for daylight and for strobe light in the night, if appropriate shutter and aperture adjustment are made.

Table 2 Precision of object coordinates of targets in the experiment

Standard deviations (mm)			
X	Y	Z	rms
0.287	0.193	0.256	0.248

At the second epoch of time twenty images are exposed with the same configuration as in the first epoch. Between the two epochs one target Target21, shown enclosed with a circle in Fig.4, is hammered down by about 5mm. Adjustment result is almost the same as in Table 4.

The result of displacement detection of targets is shown in Fig.6. The upper left window of the figure shows estimated displacements of each target (X in blue, Y in green and Z in red), the upper center shows T_X values in (18) and the upper right shows the occurring probabilities. According to the left window, 1.0-1.5 mm displacement in Y and 3mm in Z can be detected, which is better than in simulation. The displacement of five mm at Target 21 is accurately retrieved. The value of T_X at Target21 is very large compared to other perturbation, so that the occurring probability is 100%.

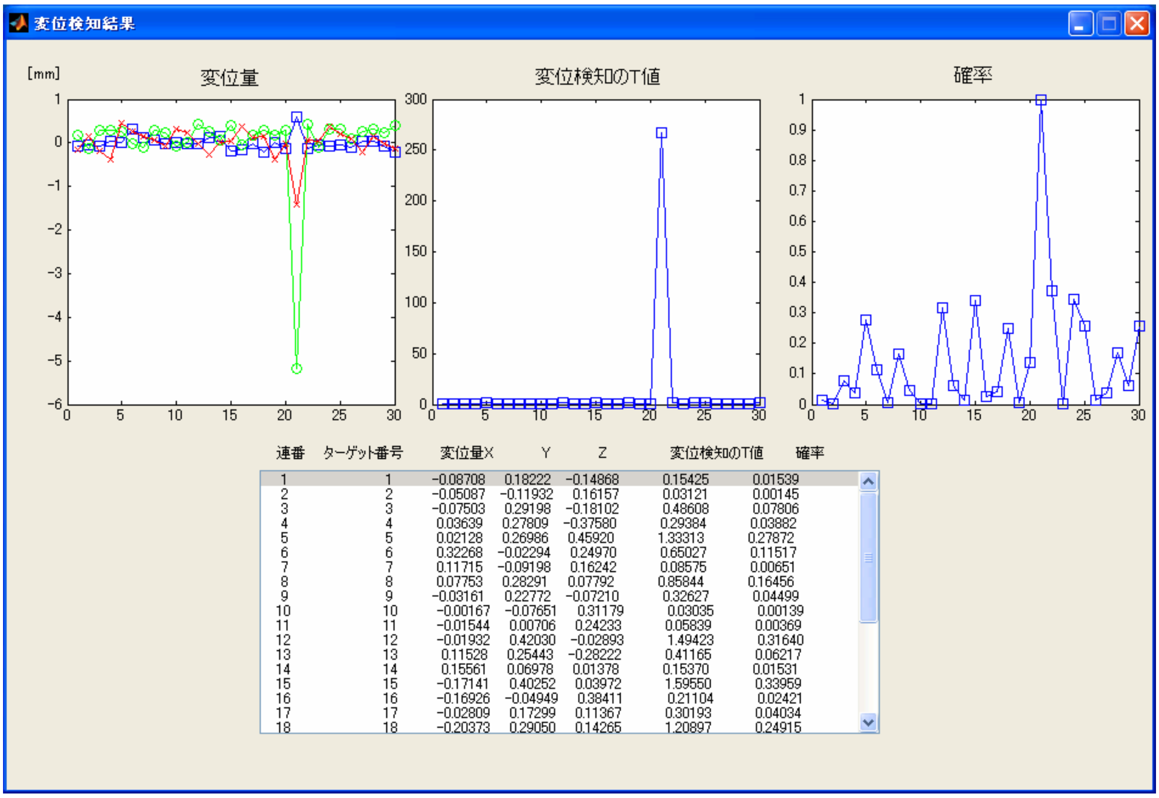

連番	ターゲット番号	変位量X	Y	Z	変位検知のT値	確率
1	1	−0.08708	0.18222	−0.14868	0.15425	0.01539
2	2	−0.05087	−0.11932	0.16157	0.03121	0.00145
3	3	−0.07503	0.29198	−0.18102	0.48608	0.07806
4	4	0.03639	0.27809	−0.37580	0.29384	0.03882
5	5	0.02128	0.26986	0.45920	1.33313	0.27872
6	6	0.32268	−0.02294	0.24970	0.65027	0.11517
7	7	0.11715	−0.09198	0.16242	0.08575	0.00651
8	8	0.07753	0.28291	0.07792	0.85844	0.16456
9	9	−0.03161	0.22772	−0.07210	0.32627	0.04499
10	10	−0.00167	−0.07651	0.31179	0.03035	0.00139
11	11	−0.01544	0.00706	0.24233	0.05839	0.00369
12	12	−0.01932	0.42030	−0.02893	1.49423	0.31640
13	13	0.11528	0.25443	−0.28222	0.41165	0.06217
14	14	0.15561	0.06978	0.01378	0.15370	0.01531
15	15	−0.17141	0.40252	0.03972	1.59550	0.33959
16	16	−0.16926	−0.04949	0.38411	0.21104	0.02421
17	17	−0.02809	0.17299	0.11367	0.30193	0.04034
18	18	−0.20373	0.29050	0.14265	1.20897	0.24915

Fig. 6 Estimated displacements and their occurring probabilities

6. CONCLUSION

The paper discusses the mathematical formulation of photogrammetric adjustment and hypothetical test procedures on displacement detection. An object space of targets placed on a slope is exposed at two epochs of time. All the image coordinates are simultaneously bundle-adjusted to find out whether any target is displaced between epochs. And the paper also refers to the development of a simulator for photogrammetric network design. An experiment and a related simulation are conducted to validate the discussions.

REFERENCES

1) Baarda, W, 1968; A Testing Procedure for Use in Geodetic Networks, Netherland Geodetic Commission, New Series 2, No.5, Delft
2)Brown,D.C,1966; Decentering Distorsion of Lenses, Photogrammetric Engineering, Vol.32,No.3,pp.444-462
3) Benzao,T. and Z.Shaorong,1995; Optical Design of Monitoring Networks with Prior Deformation Information, Survey Review, pp.33-258
4) Hattori, Susumu, K.Akimoto and et.al., 2002; Automated Procedures with Coded Targetgs in Industrial Vision Metrology, PE&RS, Vol.68,No.5,pp.441-446, May 2002
5) Koch, K. Rudolf. 1999; Parameter Estimation and Hypothesis Testing in Linear Models, Springer, 279-282, Berlin,
6) Miura S., S. Hattori et.al., 2004: Deformation Monitoring of a Slope by Vision Metrology, XX ISPRS2004, Commission5, Paper No.523, Istanbul
7) Suzuki, N. et.al., 2007: Outdoor experiments on the deformation measurement system by electromagnetic phase difference, Electronic, information and communication society, B-2-28, (in Japanese)

BIOGRAPHICAL NOTES

Susumu Hattori (Doctor) is a professor of department of Information Science in Fukuyama University. His interest is photogrammetry and computer vision, He runs a venture company "Vision Metrology Laboratory" or VML.
Yoshiyuki Ohnishi (Master) is a research assistant and a computer programmer in VML
Izuru Kuronuma (Master) is a researcher in Advanced Technology Department, Research Center, Kajima corp.

CONTACTS

Prof. Susumu Hattori
Fukuyama University
Gakuencho 1
Fukuyama City
Japan
Tel. +81-84-936-2111 ext 4765
Fax + 81-84-936-0080
Email: hattori@fuip.fukuyama-u.ac.jp
http://www.gazokeisoku.co.jp